# Millimeter Wave Wideband Communication Performance for Various Corridors

**Chien-Ching Chiu and Chi-Ping Wang**
**Department of Electrical Engineering, Tamkang University,**
**Tamsui, Taiwan, R.O.C.**

## Abstract

A comparison of wideband communication characteristics for five different geometrical configurations of corridors at 57.5 GHz is investigated. Shooting and bouncing ray/images techniques are applied to compute the impulse responses for : (i) the straight shape corridor with rectangular cross section (ii) the straight shape corridor with arched cross section (iii) the curved shape corridor with rectangular cross section (iv) the curved shape corridor with arched cross section and (v) the L-shape corridor. By using the impulse responses of these multipath channels, the outage probabilities for high-speed BPSK(binary phase shift keying) systems with phase and timing recovery circuits are calculated. Numerical results show that the outage probability for the L-shape corridor is the largest among all the five configurations being studied. Also, the outage probabilities for the arched cross section corridors are smaller than those for the rectangular cross section corridors regardless of the shapes. In addition, the effect of space antenna diversity techniques on mitigating the multipath fading is also investigated.

## I. Introduction

Design of high quality, high speed wireless networks to connect mobile users, aiming at hundred Mbps, requires large bandwidth availability. For this reason and with the aim of implementing new wireless systems, special attention has been paid to millimeter-wave networks based on short range communication.

Among the wide millimeter-wave frequency band, the frequency band around 60 GHz atmospheric oxygen absorption band seems very promising due to the large spectrum availability and the cell planning flexibility, in fact, the cell layout is practically coincident with room topology on account of large wall transmission attenuation. In recent years, a few research efforts on exploring the use of this frequency band for indoor communication systems have been reported [1]-[3]. For corridors, however, most papers are dealt with straight shape corridors of rectangular cross section. In reality, some corridors in our daily life are not straight and not with rectangular cross section. Detailed understanding of the radio propagation characteristics in various corridors of different shapes and cross sections will help the design of personal communication service systems. In this paper, a comparison of wideband communication characteristics for five different geometrical configurations of corridors at 57.5 GHz is investigated. Channel modeling for various corridors and system description is given in section II. Section III shows the numerical results. Finally, some conclusions are drawn in section IV.

## II. Channel Modeling and System Description

(A) Channel Modeling

The equation used to model the multipath radio channel is a linear filter with an equivalent baseband impulse response given by

$$h_b(\tau)=\sum_{K=0}^{N}\beta_k e^{i\theta_k}\delta(\tau-\tau_k) \qquad (1)$$

where k is the path index, $\beta_k$ is the path gain, $\theta_k$ is the phase shift and $\tau_k$ is the time delay of the kth path. $\delta(\,)$ is the Dirac delta function [4]. The goal of channel modeling is to determine the $\beta_k$'s, $\theta_k$'s, and $\tau_k$'s for any transmitter-receiver location in the building.

Let us consider five different geometrical configurations of corridors as shown in Fig. 1. The boundaries of these corridors are composed of triangular facets. The frequency transfer



0-7803-3871-5/97/$10.00 © 1997 IEEE

function of each corridor for any transmitter-receiver location is computed by the shooting and bouncing ray/image (SBR/Image) techniques [5]. The SBR/Image method can deal with high frequency radio wave propagation in complex indoor environments. It conceptually assumes that many triangular ray tubes (not rays) are shot from the transmitter and each ray tube bouncing and penetrating in the environments is traced. If the receiver is within a ray tube, the ray tube will

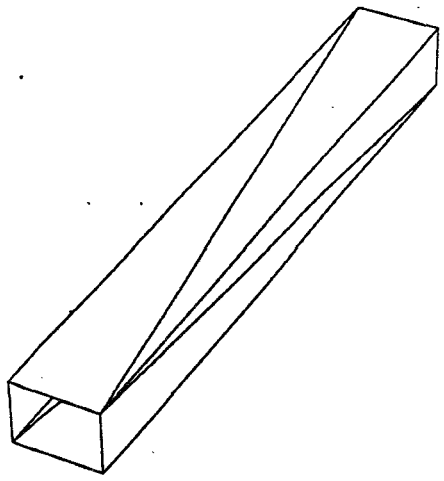

Fig. 1(a)

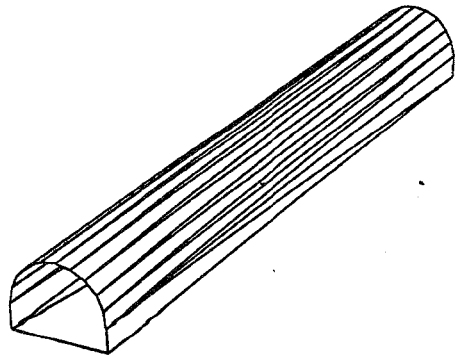

Fig. 1(b)

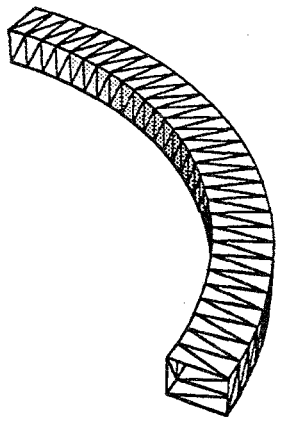

Fig. 1(c)

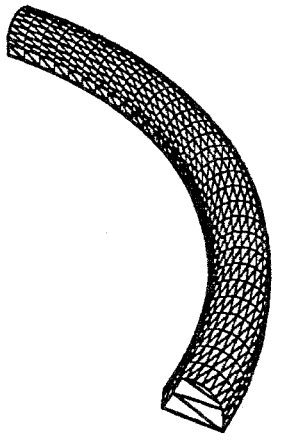

Fig. 1(d)

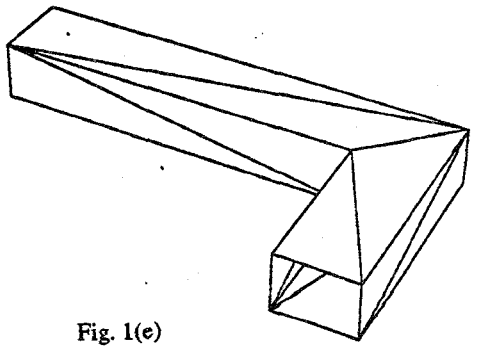

Fig. 1(e)

Fig. 1 Five different geometrical configurations of corridors modeled by triangular facets.

have contribution to the received field and the corresponding equivalent source (image) can be determined. By summing all contributions of these images, we can obtain the total received fields at the receiving antenna for any given carrier frequency. The complex frequency transfer function can be obtained by sweeping the frequency. Then, the impulse response of the channel in the time domain, $h_{rf}(t)$, is obtained by applying inverse Fourier transform to this frequency transfer function. As a result, the parameters $\beta_k$, $\theta_k$, and $\tau_k$ in Eq. (1) for the equivalent baseband impulse response, $h_b(t)$, can be obtained. Note that $h_{rf}(t)$ is equal to $h_b(t)e^{i\omega_c t}$, where $\omega_c$ is the angular carrier frequency.

(B) System description

A BPSK (binary phase shift keying) system with raised cosine pulse shaping (rolloff factor $\alpha$), phase and timing recovery circuits is considered. The equivalent baseband channel models are plotted in Fig. 2. In Fig. 2, $h_t(t)$ and $h_r(t)$ represent the transmitting waveform and the receiving filter respectively. They are both chosen as the impulse responses of the square root of the raised cosine function with rolloff factor $\alpha$=0.5. $h_b(t)$ is the equivalent baseband impulse response of multipath propagation for any transmitter-receiver location. n(t) is the zero-mean additive white Gaussian noise. $a_n$ is the transmitted binary data and T is the transmitted interval of data.

In the phase recovery circuit, the near optimum remodulation scheme suggested in [6] is used. In this method, the phase of the overall complex channel impulse response is used as the phase reference. Moreover, a squaring-enveloped scheme is used for timing recovery circuit [7]. The circuit consists of a square-raw envelope detector and a narrowband filter extracting the spectral line at frequency $\frac{1}{T}$.

Given the phase and timing recovery, the probability of error for this BPSK system can be calculated by the method described in reference [8].

## III. Numerical results

Let us consider five different geometrical configurations of corridors as shown in Fig. 1. The cross sections of all corridors are 4 m wide and 3 m high. The length of the straight shape corridors, the radius of the curved shape corridors and the total length of the L-shape corridor are all 30 m. Also, the circumference of the curved corridors is about 47 m. 25 cm-thick concrete floors with refractive index n=2.55-0.084i, and 15 cm-thick plasterboard walls and ceilings with refractive index n=1.76-0.014i are assumed for these corridors [3]. Half-wave dipole antennas with vertical polarization are used for both transmission and reception. The transmitting antenna (Tx) is located at the corner of the corridors with a fixed height of 2.5 m. The locations of receiving antennas (Rx) are uniformly distributed inside the corridors with a fixed height of 1.5 m. There are 1000 receiving points for each corridor.

The complex frequency transfer function for each channel was calculated over 1 GHz band

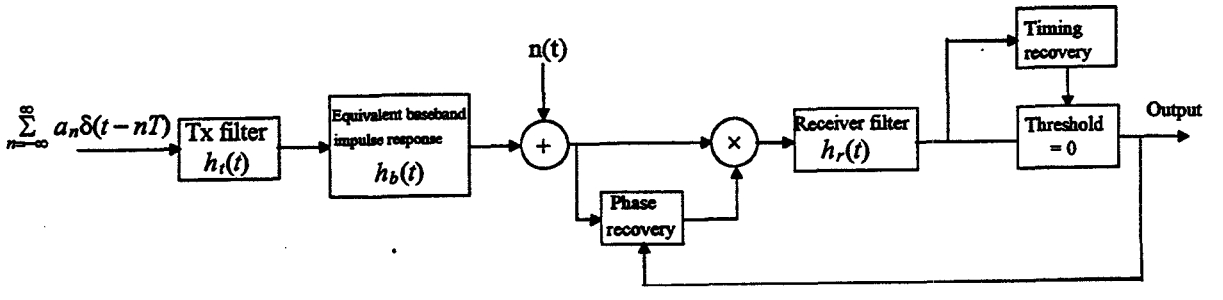


Fig. 2 Block diagrams of the equivalent baseband communication system.

centered at 57.5 GHz by SBR/Image method. The maximum number of bounces setting beforehand is 10, and the convergence is confirmed. Since the extra attenuation at 57.5 GHz due to atmospheric absorption and scattering is negligible over small distance, the atmospheric attenuation is not considered in the simulation [2]. By applying the inverse Fourier transform to the frequency transfer function, the impulse response in the time domain can be obtained.

The cumulative distributions of the root mean square (rms) delay spreads for these five corridors are plotted in Fig. 3. Besides, the means and standard deviations of the rms delay spreads for these corridors are shown in Table 1. It is clearly seen that the multipath effect for the L-shape corridor is the most severe; Meanwhile, the rms delay spreads for LOS cases is larger than those for the OOS cases in this L-shape corridor. This is due to the fact that the multipath effect caused by the back wall for LOS cases is severe. From Fig. 3(a) and Table 1, it is also found that the mean rms delay spreads for the arched cross section corridors are lower than those for the rectangular cross section corridors regardless of the shapes. This phenomenon can be explained by the fact that the multipath effect for the arched cross section corridors is less severe than those for the rectangular cross section corridors.

Next, let us consider the BER (bit error rate) performance for these corridors. The BERs at 100 Mbps and SNR (signal to noise ratio) = 30 dB are calculated. Here SNR is defined as the ratio of the average power $S_{av}$ to the noise power at the front end of the receiver. The calculated BERs are used to compute the outage probability. For the BER requirement of BER<$10^{-5}$, the outage probabilities for the five specific corridors in Fig. 1 are also depicted in Table 1. From Table 1, it is seen that the outage probability for the L-shape corridor is the largest. Moreover, the outage probabilities for the arched cross section are smaller than those for the rectangular cross section regardless of the shapes. These results are coincident with the mean rms delay spread values for these five corridors.

In order to reduce the outage probabilities, the dual space antenna diversity system is employed to counteracting the multipath fading. Here, a post detection scheme and selecting combining are used in the system. For each receiving point, two antennas separated by 4.2 cm are used to receive the signal. It is found that the outage probability is reduced from 12% to 1.8% for the curved shape corridor with rectangular cross section. This indicates that the bit rate of 100 Mbps is feasible for curved shape corridor with rectangular cross section by applying space antenna diversity technique if 2% outage probability is considered as acceptable.

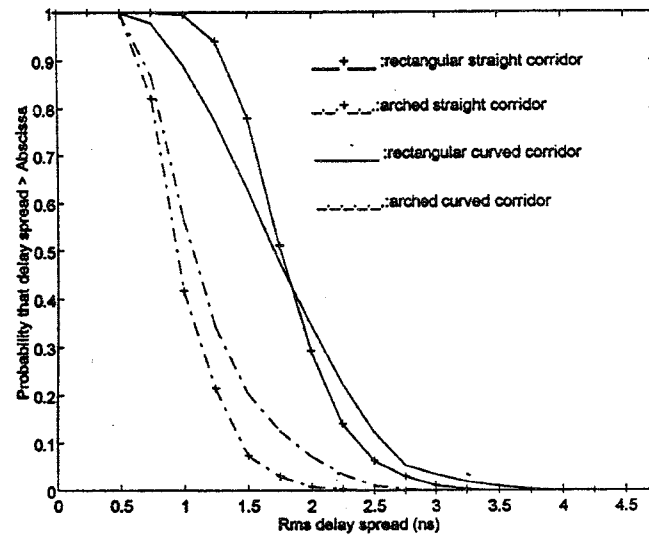


Fig. 3(a)

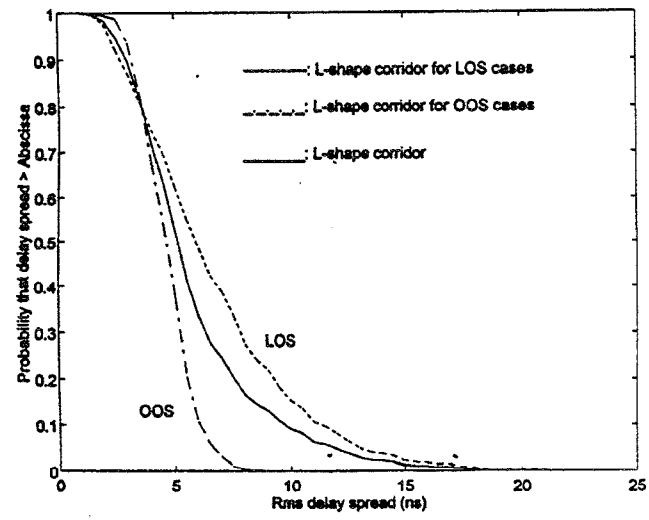


Fig. 3(b)

Fig. 3 Cumulative distributions of rms delay spreads for the five different geometrical configurations of corridors.
(a) straight and curved shapes corridorswith rectangular and arched cross sections.
(b) L-shape corridor.

Table. 1 Rms delay spread (mean and standard deviation) and outage probabilities for the five different geometrical configurations of corridors.

| Parameters / Shapes | Rms delay spread $\tau_{rms}$ | | Outage probability |
|---|---|---|---|
| | mean | standard deviation | |
| Rectangular straight corridor | 1.82 ns | 0.42 ns | 17 % |
| Arched straight corridor | 1.02 ns | 0.30 ns | 8 % |
| Rectangular curved corridor | 1.77 ns | 0.67 ns | 12 % |
| Arched curved corridor | 1.18 ns | 0.48 ns | 7 % |
| L-shape corridor | 5.82 ns | 3.57 ns | 26 % |

Similar results have been obtained for the other three configurations except the L-shape corridor. For the L-shape corridor, the outage probability is still too high (9.8%). This phenomenon can be explained by the severe multipath effect of this type of corridor.

## IV. Conclusions

A comparison of wideband communication characteristics for corridors of different shapes and cross sections at 57.5 GHz is presented. The impulse responses of the channels are computed by SBR/Image method and Fourier transform. By using the impulse responses of the multipath channels, the outage probabilities for 100 Mbps high-speed BPSK communication systems with phase and timing recovery circuits have been calculated. It is found that the outage probability for the L-shape corridor is the largest. Besides, the outage probabilities for the rectangular cross section corridors are larger than those for the arched cross section corridors regardless of the shapes. Moreover, the effect of space antenna diversity techniques on mitigating multipath fading is also investigated. Numerical results show that 100 Mbps transmission rate is feasible for both the straight and curved shapes corridors by applying space antenna diversity techniques.

## Acknowledgment

This work was supported by National Science Council, Republic of China, under Grant NSC-86-2221-E-032-003. The author would like to thank Dr. S. K. Jeng and Dr. S. H. Chen for providing the source code of the SBR/Image method.

## References

[1] T. Manabe, K. Sato, H. Masuzawa, K. Taira, T. Ihara, Y. kasashima and K. Yamaki, "Polarization dependence of multipath propagation and high-speed transmission characteristics of indoor millimeter-wave channel at 60 GHz," *IEEE Trans. Veh. Technol.*, Vol. 44, pp. 268-274, May 1995.

[2] A. M. Hammoudeh and G. Allen, "Millimetric wavelengths radiowave propagation for line-of-sight indoor microcellular mobile communications," *IEEE Trans. Veh. Technol.*, vol. 44, pp. 449-460, Aug. 1995.

[3] D. Dardari, L. Minelli, V. Tralli and O. Andrisano, "Widband indoor communication channels at 60 GHz," *Proc. IEEE International Symposium on Personal, Indoor and Mobile Radio Communications*, vol. 3, pp. 791-794, Oct. 1996.

[4] A. A. M. Saleh and R. A. Valenzuela, "A statistical model for indoor multipath propagation," *IEEE J. Select. Areas Commun.*, vol. 5, pp. 128-137, Feb. 1987.

[5] S. H. Chen and S. K. Jeng, "SBR image approach for radio wave propagation in tunnels with and without traffic," *IEEE Trans. Veh. Technol.*, vol. 45, pp. 570-578, Aug. 1996.

[6] L. J. Greenstein and B. A. Czekaj-Augun, " Performance comparisons among digital radio techniques subjected to multipath fading," *IEEE Trans. Commun.*, vol. 30, pp. 1184-1197, May 1982.

[7] J. C. Chuang, "The effects of multipath delay spread on timing recovery," *IEEE Tran. Veh. Technol.*, vol. 35, pp. 135-140, Aug. 1987.

[8] K. Pahlavan, "Comparison between the performance of QPSK, SQPSK, QPR, and SQPR systems over microwave LOS channels," *IEEE Trans. Commun.*, vol. 33, pp. 291-296, Mar. 1985.